Function and picosecond dynamics of bacteriorhodopsin in purple membrane at different lipidation[1] and hydration

J. Fitter[a,b,]*, S.A.W. Verclas[a,c], R.E. Lechner[c], H. Seelert[a], N.A. Dencher[a]

[a]Institut für Biochemie, TU Darmstadt, Petersenstr. 22, D-64287 Darmstadt, Germany
[b]Forschungszentrum Jülich, IBI-2, Biologische Strukturforschung, D-52425 Jülich, Germany
[c]Hahn-Meitner Institut, BENSC, Glienicker Str. 100, D-14109 Berlin, Germany

Abstract By neutron scattering experiments and time-resolved absorption spectroscopy we have investigated picosecond equilibrium fluctuations and the kinetics of the photocycle of bacteriorhodopsin (BR) in the purple membrane (PM). Natural PM samples composed of 75% BR (w/w) and 25% lipid (w/w) as well as delipidated PM having only 5% lipid (w/w) were measured at different levels of hydration. We observed a reduced 'flexibility', due to a diminished weight of stochastic large-amplitude motions occurring in the delipidated PM as compared to the natural PM. This effect is more pronounced for wet samples, indicating the importance of lipid hydration for protein dynamics. The reduced flexibility is accompanied by significantly larger time constants describing the decay of the M-intermediate. Therefore, a correlation between the dynamical behavior of the protein-lipid complex and BR function emerges.
© 1998 Federation of European Biochemical Societies.

Key words: Hydration; Internal flexibility; Delipidation; Quasielastic incoherent neutron scattering; Time-resolved absorption spectroscopy

1. Introduction

Bacteriorhodopsin (BR), which functions as a light-driven proton pump in *Halobacterium salinarum*, is one of the best characterized membrane proteins. Upon capture of a photon a conformational transition from the all-*trans* to the 13-*cis* isomer of the chromophore retinal initiates a photocycle characterized by spectroscopic intermediates (for a review see [1]). As the only protein in the purple membrane (PM) BR forms together with lipids a highly ordered two-dimensional hexagonal lattice of BR trimers. In the natural PM the content of BR is about 75% (w/w), while the remaining part of the PM consists of lipids [2]. The seven-helix membrane spanning structure of BR and the arrangement of the surrounding lipids have been studied mainly by cryo-electron microscopy [3–5]. Neutron diffraction experiments showed that the photocycle of BR is accompanied by structural changes of the order of 10% in the observed intensity up to 7 Å resolution [6]. In time-resolved X-ray diffraction experiments, these structural changes were monitored with a time resolution of a few milliseconds and correlated with the photocycle kinetics [7,8]. It is known from many studies that the amount of water molecules associated with BR and with the membrane surface has an

important effect on the dynamical behavior of the protein-lipid complex [9–12], the kinetics of the photocycle, and on the vectorial proton translocation [13–15]. In particular, fast picosecond equilibrium fluctuations are very sensitive to the hydration level. Recent neutron scattering studies with fully hydrated purple membranes report on translational diffusion of water molecules on the membrane surface [16,17], as well as the effect of solvent properties on the internal molecular motions of BR in the PM. Only a sufficient level of hydration permits a structural 'flexibility', which is assumed to be essential for the function of biological molecules [9,10]. In this context, the amount and composition of lipids in which BR is embedded are other important environmental factors for BR itself, and for the hydration of the whole protein-lipid complex. In order to elucidate the influence of lipids on the function and on the dynamics of BR, we have compared PM samples with two different lipid contents at different hydration levels. We examined the thermal equilibrium fluctuations in the PM by employing quasielastic incoherent neutron scattering (QINS). Because of the large incoherent cross section of hydrogen nuclei (~ 40 times larger than the cross section of other elements) and the fact that hydrogen atoms are distributed quasi homogeneously in biological macromolecules, this technique is a powerful tool for the study of all internal motions in the time range of 10^{-13}–10^{-10} s. Characteristic features of the photocycle (e.g. time constants of the spectroscopic intermediates) have been measured in these samples using time-resolved absorption spectroscopy. The aim of the present study was therefore, by a combination of both techniques, to investigate the protein function and picosecond dynamics and to look for correlations between both.

2. Materials and methods

2.1. Sample preparation

Patches of purple membranes were isolated from *H. salinarum* according to standard procedures [18]. Beside the natural PM with a lipid content of about 25% (w/w), we prepared delipidated PM having only 5% (w/w) of lipids. The partial removal of lipids from PM without BR solubilization was performed by a modified method according to Szundi and Stoeckenius [19]. In order to obtain partially delipidated samples the detergent 3-[(3-cholamidopropyl)dimethylamino]-1-propanesulfonate (CHAPS) (Boehringer Mannheim) was used. More details on methods are described elsewhere [20]. Similar to the natural purple membrane the delipidated PM exhibits crystallinity, characterized by a hexagonal unit cell containing a BR trimer. X-ray diffraction measurements with moderately hydrated membranes revealed that the cell parameters of 62.4 Å in the natural PM is reduced in the delipidated PM to 56.9 Å (Fitter, unpublished results). It is known from a previous diffraction study that the BR structure is identical in natural and delipidated PM [5]. Suspensions of natural and delipidated PM, having a concentration of about 25 mg BR/ml (for neutron scattering) and 8.1 mg BR/ml (for absorption spectroscopy) with pH of 7.0 and

*Corresponding author (b). Fax: (49) (2461) 2020.
E-mail: j.fitter@fz-juelich.de

[1]Analogous to the terms hydration-dehydration, which describe the process of adding and removing water solvent, we would like to introduce lipidation-delipidation for the analogous process of lipids.

6 mM imidazole, were applied to prepare samples of hydrated membrane stacks. For the purpose of neutron scattering experiments an amount of 5 ml suspension was deposited on a aluminum plate (thickness 0.2 mm, diameter 50 mm). After a short drying process with silica gel, the samples have been re-hydrated with D_2O using vapor exchange over saturated K_2SO_4 solution (corresponding to a relative humidity (r.h.) of 98% at 20°C) and over NaCl solution (75% r.h.). Finally, all samples were sealed in a circular slab-shaped aluminum container, which guaranteed constant hydration levels during the experiments. The samples for the absorption spectroscopy have been prepared using 40 µl suspension, which was deposited on a surface of quartz plates (1 cm^2). All samples were shortly dried in nitrogen atmosphere and subsequently the individual samples have been exposed for at least 24 h in H_2O atmospheres with saturated salt solution obtaining the following relative humidities: 29% [$CaCl_2$], 41% [$Zn(NO_3)_2$], 58% [NaBr], 75% [NaCl], 81% [$(NH_4)_2SO_4$], 86% [KCl], 94% [KNO_3], 98% [K_2SO_4] and 100% [pure H_2O].

2.2. Incoherent neutron scattering

Neutron scattering experiments have been carried out using the time-of-flight (TOF) spectrometer NEAT (Hahn-Meitner Institut, Berlin) [21]. TOF spectra were measured using an incident wavelength of 5.1 Å, with an elastic energy resolution of 100 µeV, and within an angular range of $13.3° \le \phi \le 136.7°$. All samples, including vanadium standard and empty can, were measured at room temperature (293 K) and with a sample orientation angle of $\alpha = 45°$ with respect to the incident neutron beam direction. The TOF spectra were corrected, normalized, grouped, and transformed to the energy transfer scale using our data analyzing program FITMO. Relatively large transmission values of $T(90°) \approx 0.93$–0.95 enabled us to perform the data analysis without a correction for multiple scattering.

Using samples hydrated in D_2O, the predominant part of the measured signal is due to incoherent scattering by the non-exchangeable hydrogen atoms. According to the stochastic character of the predominant part of the motions (in our time range), the following expression was used for the theoretical incoherent scattering function:

$$S_{theor}(\vec{Q}, \omega) = e^{-\langle u^2 \rangle Q^2} \cdot [A_0(\vec{Q} \cdot \delta(\omega) + \sum_n A_n(\vec{Q}) \cdot L_n(H_n, \omega)] \quad (1)$$

The scattered intensity is separated into an elastic $\delta(\omega)$-shaped component and quasielastic Lorentzian-shaped contributions $L_n(H_n, \omega)$, parameterized by the width $H_n = (\tau_n)^{-1}$ (τ_n are the corresponding correlation times) and the quasielastic incoherent structure factors A_n. The amplitude of the elastic component is given by the elastic incoherent structure factor (EISF) A_0. Faster motions are taken into account by the Debye-Waller factor, where $\langle u^2 \rangle$ gives the global averaged 'mean square displacements' of vibrational motions. As already known from previous dynamic studies, the major part of the scattering is due to local diffusive motions of hydrogen atoms within restricted volumes (with a size of a few Å) and with correlation times of 0.1–100 ps [10,22]. A convenient phenomenological description, which should reproduce some more general properties of the complex dynamical behavior, is provided by a model, developed by Volino and Dianoux [23]. It describes free diffusion inside the volume of a sphere with the radius r, where the EISF is given by

$$A_0(\vec{Q}) = \left[3 \frac{\sin(Qr) - (Qr) \cdot \cos(Qr)}{(Qr)^3}\right]^2 \quad (2)$$

Because our data are limited in momentum transfer Q (with $Q_{max} = 2.25$ Å) and we used only an energy transfer range with $|\hbar\omega| \le 0.8$ meV, we need to consider only the first quasielastic component. Therefore, the theoretical scattering function is only parameterized by r (determining A_0 and $A_1 = 1 - A_0$) and the width of the quasielastic contribution $H_1 = (\tau_1)^{-1}$. For more details on methods see for example [22,24].

In the case of biological macromolecules, the correlation times τ_1 and radii r must be understood as values averaged over all the motions observable in the time window of our experiments (a few picoseconds). The theoretical scattering function was fitted to the measured scattering function using the following relation:

$$S_{meas}(\vec{Q}, \omega) = F \cdot e^{\frac{-\hbar\omega}{2k_BT}} \cdot [S_{theor}(\vec{Q}, \omega) \otimes S_{res}(\vec{Q}, \omega)] + B \quad (3)$$

where a convolution with the resolution function $S_{res}(Q, \omega)$ (obtained from vanadium measurements) and factors, such as the normalization factor F, the detailed balance factor $\exp(-\hbar\omega/2k_BT)$, and a linear 'background' B have been applied.

2.3. Time-resolved absorption spectroscopy

The time-resolved absorption spectroscopy allows the measurement of the transient absorption changes from bacteriorhodopsin after a pulsed laser stimulation. The measurements have been performed using a transient absorption spectrometer, which was described in detail elsewhere [15]. The transient absorption changes were monitored at room temperature (293 K) in a time range of 10^{-8}–10^{+2} s. After light absorption, bacteriorhodopsin undergoes a photocycle, passing a series of intermediates with characteristic protein-chromophore states and characteristic absorption spectra (see for example [25]).

$$BR + h\nu \rightarrow J \leftrightarrow K \leftrightarrow L \leftrightarrow M_1 \rightarrow M_2 \leftrightarrow N \leftrightarrow O \rightarrow BR \quad (4)$$
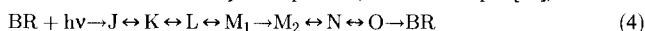
The most prominent intermediate is the M-intermediate, which is directly correlated with the proton release event. This intermediate is characterized by a blue-shifted absorption maximum at 412 nm in comparison with the maximum of the ground state at 568 nm. The two spectroscopic substates M_1 and M_2 cannot be separated by spectroscopic visible light absorption methods; thus, here they will be represented by only one M-intermediate. The time-resolved M-signal, i.e. the absorption changes at 412 nm after a laser flash, can be taken as a simplified representation for the whole photocycle. The evaluation of the M-signal was done by fitting a sum of n exponentials to the measured data, where n is the number of the intermediates. In general, the time-resolved absorption changes ΔA at the wavelength λ can be described by the following equation, in which the time constants τ_{Mi} characterize the transitions between the intermediates:

$$\Delta A(\lambda, t) = \sum_{i=1}^{n} a_i \cdot \exp(-t/\tau_{Mi}) \quad (5)$$

With respect to the six intermediates, which can be separated by spectroscopic methods, we used in the present study a sum of $n = 6$ exponentials guaranteeing a sufficiently good fit quality of the time resolved M-signal.

3. Results and discussion

As already mentioned, the internal motions on the picosecond time scale are mainly stochastic reorientations of molecular subunits, such as polypeptide side groups or fatty acid chains [22,26]. These kinds of motions are restricted to limited volumes (as described by our model). As a consequence of this, and in the case of a limited energy transfer range, we were able to fit all data with only one quasielastic component having a Q independent line width of $H = 150$ µeV, which corresponds to a correlation time of $\tau_1 = 4.4$ ps. Since we are dealing with very complex biological macromolecules performing various and different types of molecular motions, the obtained correlation time τ_1 and the radius r must be understood as 'mean' values. Examples of the fit quality and the resulting parameters of the fits are shown in Fig. 1. The radii r, determining the volume of the stochastic reorientational motions, can be interpreted as 'amplitudes' of these motions. These 'large amplitude' motions give the main contribution to what we will call 'internal flexibility'. The averaged 'mean square displacements' $\langle u^2 \rangle$ represent amplitudes of mainly vibrational motions. The comparison of internal molecular motions occurring in natural PM and in delipidated PM samples revealed the following results.

(1) We find more internal flexibility, related to more quasielastic scattering with larger radii r and to larger $\langle u^2 \rangle$, in natural PM as compared to delipidated PM (see inserted box in Fig. 1). As shown in the inserted graphs of Fig. 1, a steeper decrease of the A_0 with Q is related to larger 'ampli-
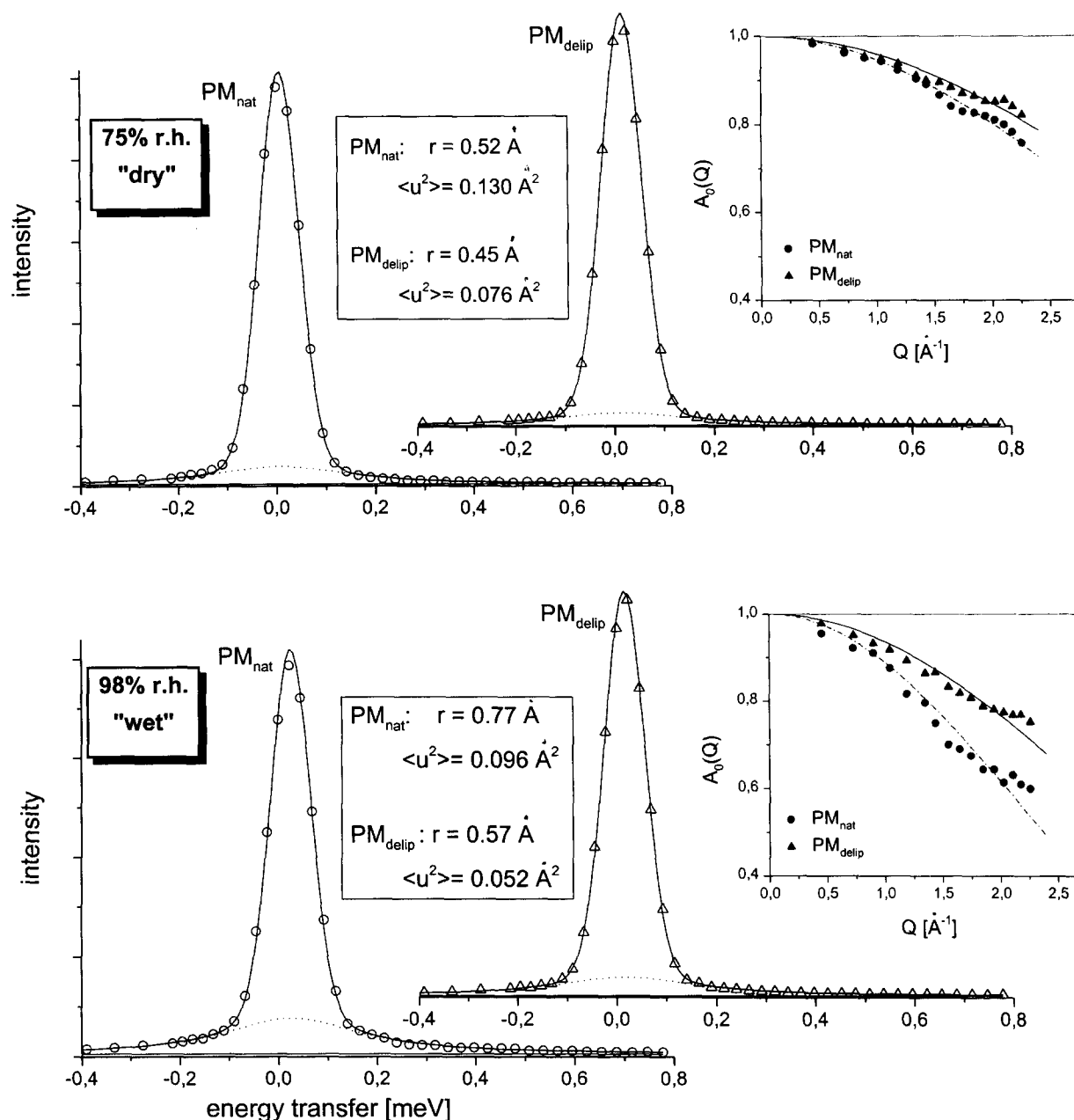
Fig. 1. Comparison of TOF spectra measured with natural and delipidated PM samples at two different hydration levels. The spectra shown in this figure have been measured at a scattering angle of $\phi = 90.5°$. The total scattering function which fits the experimental points (open symbols) is composed of an elastic component (represented by the area between fitting solid line and dotted line), a quasielastic component (area between dotted line and solid background line) and a linear background (solid line). Inserted graph: The experimental EISF (A_0) (solid symbols) as obtained from fits are shown as a function of momentum transfer Q. For this purpose, all 16 spectra have been fitted separately with radius r as a free parameter. The statistical error of the experimental EISF is approximately ± 0.015, which is about the size of the symbols. The corresponding theoretical EISF (PM$_{nat}$: dashed-dotted line, PM$_{delip}$ solid line) were obtained from fits, where all spectra have been fitted simultaneously. Inserted box: The given radii r and averaged 'mean square displacements' $\langle u^2 \rangle$ are the parameters resulting from these fits.

tudes' r and therefore to a larger internal flexibility. The difference in flexibility between natural and delipidated PM is relatively weak in the case of 'dry' (75% r.h.) samples and more pronounced in the case of 'wet' (98% r.h.) samples (Fig. 1).

(2) With respect to the obtained radii r, and as already known from previous studies, 'wet' samples exhibit more internal flexibility than 'dry' samples. This effect is more pronounced in the case of natural PM samples as compared to delipidated PM samples. Due to damping of the vibrational

motions in wet samples, the mean square displacements $\langle u^2 \rangle$ are smaller as compared to dry samples (Fig. 1).

Because the samples were hydrated with D$_2$O (solvent scattering at 100% r.h. is about 3.6% of the total scattering and less at lower hydration levels), we do not observe the dynamics of the solvent itself, but the effect of solvent on the dynamics of the protein-lipid complex. Furthermore, the results indicate that either the lipids themselves are more flexible than the membrane protein BR (a high lipid content leads to an increased 'overall' internal flexibility in the PM as compared
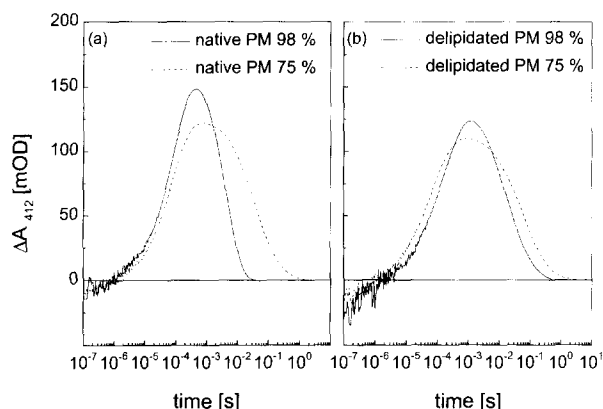
Fig. 2. Time-resolved absorption changes of the M-intermediate as measured with (a) natural and (b) delipidated PM samples. For each relative humidity the curve shown was obtained by adding up 20 consecutive absorption change measurements performed under constant conditions (constant temperature and relative humidity) and with a sampling rate of 10^8 s^{-1}. For times longer than 10^{-5} s the statistical error of the given absorption changes is 1–2%.

to a low lipid content), or that more lipids increase the flexibility of the membrane proteins. A further, and most probable, possibility is a combination of both influences. It is reasonable to assume that in the tightly packed protein-lipid complex the dynamics of BR is coupled with the dynamics of the lipids. The fact that the differences in the flexibility between natural and delipidated PM samples are much more pronounced in 'wet' samples, gives strong evidence that mainly the presence of hydration water, which is attached to the polar lipid headgroups at high hydration levels, increases the internal flexibility of the protein-lipid complex. This hypothesis is supported by diffraction experiments performed with natural PM, where at high hydration levels a larger in-plane cell parameter was found (62.4 Å) as compared to dry samples (61.4 Å). The reduction of the in-plane cell dimension is related to a removal of solvent molecules which were around the lipid headgroups [27,28]. Although, on the basis of the present data, we are not able to distinguish between dynamics of the lipids and dynamics of BR, we can draw the conclusion that the amount of lipids and their ability to attract solvent molecules is strongly related to 'large amplitude' motions of the whole purple membrane [29].

The influence of hydration and of lipid content on the kinetics of the photocycle of BR has been investigated by time-resolved absorption spectroscopy of the M-intermediate. A comparison of time-resolved absorption changes for two relative humidities (75% and 98% r.h.) is shown in Fig. 2. With respect to the natural PM sample hydrated at 98% r.h. the 75% sample (Fig. 2a) is characterized by a small shift to longer times for the M-formation (rise of the curve), while the M-decay (decent of the curve) is strongly shifted to longer times. In the case of delipidated PM samples, the M-formation of the 75% sample is shifted to shorter times as compared to the 98% sample. The M-decay is similar to the natural PM characterized by a shift to longer times[2]. A quantitative characterization of the M-absorption kinetics for the natural and the delipidated PM is given, according to Eq. 5, by the corresponding time constants, shown as a function of all measured

relative humidities (see Fig. 3). The time constants τ_{M1}–τ_{M3} are attributed to the M-formation, while the time constants τ_{M4}–τ_{M6} are characterizing the M-decay. The following features are represented by the data:

With respect to the hydration level the M-decay of both the natural and delipidated PM is affected only between 100% and 75% r.h. In the case of natural PM the M-decay is prolonged approximately by an order of magnitude going from 100% to 75% r.h.. In contrast to natural PM samples, the prolongation of the M-decay between 100% and 75% r.h. is much less pronounced in delipidated samples, because their decay time constant is much larger already at full hydration. At hydration levels below 75% r.h. the M-decay is similar and no more dependent on the hydration level for both, the natural and the delipidated PM. Within the limits of error the M-formation kinetics of delipidated samples is not affected by the hydration level. The hydration dependence of the M-formation in the case of natural PM is more complex. With respect to the delipidated PM, the natural PM shows between 100% and 75% r.h. a τ_{M1} which is smaller (and slightly increasing), while τ_{M2} and τ_{M3} values coincide with those observed in delipidated samples. Natural PM samples exhibit larger time constants (τ_{M1}–τ_{M3}) at 58% r.h. and smaller time constants at 29% r.h. as compared to delipidated PM.

Similar observations of the effect of hydration on the one hand [13,15] and the effect of lipidation on the other hand
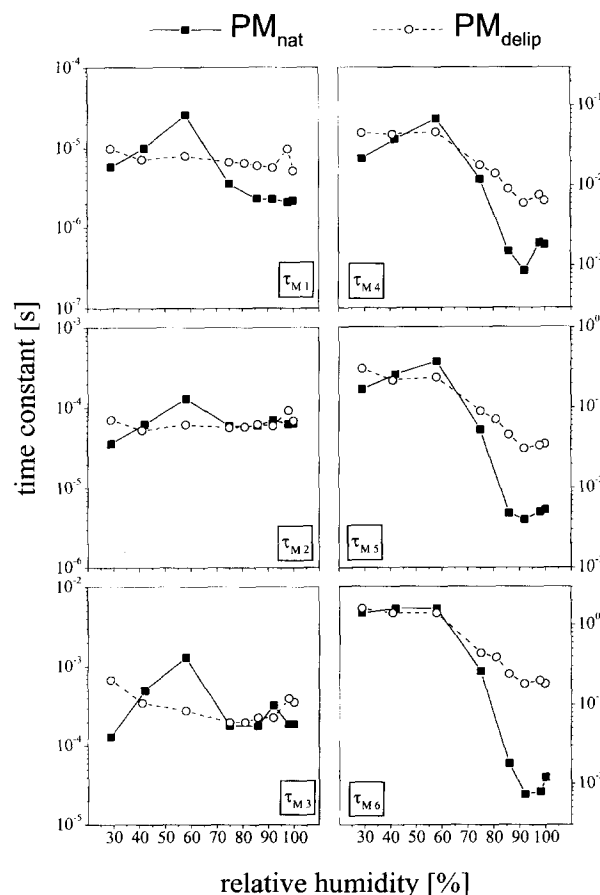

relative humidity [%]

Fig. 3. Time constants characterizing the absorption signal of the M-intermediate in natural PM (squares) and in delipidated PM (circles) as a function of relative humidity. Time constants τ_{M1}–τ_{M3} represent the M-formation, while τ_{M4}–τ_{M6} relate to the decay of the M-intermediate.

---

[2] Note that the logarithmic time scale 'overestimates' absorption differences at short times.

[30,31], have already been reported previously. The combination of measurements using samples at different hydration levels and different lipidations, as performed in the present work for the first time, shows further that the kinetics of the M-decay is only significantly different for both lipid concentrations at hydration levels higher than 75% r.h. Supporting the central idea of dynamics-function correlation, the time constants related to the M-decay and the parameters describing the internal flexibility (Fig. 1) also differ only at high hydration levels for both lipid concentrations. As shown in recently published diffraction studies, the prominent tertiary structural change [6,7], which is supposed to occur during the $M_1 \rightarrow M_2$ transition, is inhibited at hydration levels below 75% r.h. [11]. Asking for the reason of the prolonged M-decay at low hydration levels, which seems be related to hindering of the $M_1 \rightarrow M_2$ transition, mainly two explanations were proposed in the literature [32–34]: (1) the removal of essential water molecules (as part of the proposed proton pathway) located in the interior of BR, (2) reduced flexibility of the protein structure. Recent studies on PM using pH-sensitive dyes, revealed that BR in delipidated (partially delipidated as used in this present study) and fully hydrated PM is active as a light-driven proton pump [35]. The rate of proton transfer from the Schiff base to the extra-cellular BR surface is not altered by delipidation, however, the surface to bulk equilibration rate is slowed down by a factor of about 7. On the other hand, proton re-uptake is dramatically slowed down in the delipidated PM. The overall proton transfer process from the cytoplasmic surface to the Schiff base is decelerated 17 times, whereas the bulk to surface transfer is retarded even by a factor of 37.

In the present work we found a prolonged M-decay in the fully hydrated but delipidated PM samples[3], where no water molecules attached to the BR molecule are removed. Therefore, this supports the following concept: internal fast stochastic and large amplitude motions occurring in BR (or in the PM) are strongly related to the hydration of the lipid phase. These motions are essential (in the sense of a 'lubricant') for slower (micro- to millisecond time scale) conformational changes, which are directly related to the vectorial proton translocation.

References

[1] Oesterhelt, D. and Tittor, J. (1989) Trends Biochem. Sci. 14, 57–61.

[2] Kates, M., Kushwaha, S.C. and Sprott, G.D. (1982) Methods Enzymol. 88, 98–111.

[3] Grigorieff, N., Cheska, T.A., Downing, K.H. and Henderson, R. (1996) J. Mol. Biol. 259, 393–421.

[4] Glaeser, R.M., Jubb, J.S. and Henderson, R. (1985) Biophys. J. 48, 775–780.

[5] Grigorieff, N., Beckmann, E. and Zemlin, F. (1995) J. Mol. Biol. 254, 404–415.

[6] Dencher, N.A., Dresselhaus, D., Zaccai, G. and Büldt, G. (1989) Proc. Natl. Acad. Sci. USA 90, 9669–9672.

[7] Koch, M.H.J., Dencher, N.A., Oesterhelt, D., Plöhn, H.-J., Rapp, G. and Büldt, G. (1990) EMBO J. 10, 521–526.

[8] Dencher, N.A., Heberle, J., Bark, C., Koch, M.H.J., Rapp, G., Oesterhelt, D., Bartels, K. and Büldt, G. (1991) Photochem. Photobiol. 54, 881–887.

[9] Ferrand, M., Dianoux, A.J., Petry, W. and Zaccai, G. (1993) Proc. Natl. Acad. Sci. USA 90, 9668–9672.

[10] Fitter, J., Lechner, R.E. and Dencher, N.A. (1997) Biophys. J. 73, 2126–2137.

[11] Saß, H.-J., Schachowa, I., Rapp, G., Koch, M.H.J., Oesterhelt, D., Büldt, G. and Dencher, N.A. (1997) EMBO J. 16, 1484–1491.

[12] Lechner, R.E., Fitter, J., Dencher, N.A. and Hauß, Th. (1998) J. Mol. Biol. 277, 593–603.

[13] Korenstein, R. and Hess, B. (1977) Nature 270, 184–186.

[14] Hauß, Th., Papadopoulos, G., Veclas, S.A.W., Büldt, G. and Dencher, N.A. (1997) Physica B 234/236, 217–219.

[15] Tiedemann, G., Heberle, J. and Dencher, N.A. (1992) in: Structures and Function of Retinal Proteins (Rigaud, J.L., Ed.), pp. 217–220, Libbey Eurotext, Montrouge.

[16] Lechner, R.E., Dencher, N.A., Fitter, J., Büldt, G. and Belushkin, A.V. (1994) Biophys. Chem. 49, 91–99.

[17] Lechner, R.E., Dencher, N.A., Fitter, J. and Dippel, Th. (1994) Solid State Ionics 70/71, 296–304.

[18] Bauer, P.J., Dencher, N.A. and Heyn, M. (1976) Biophys. Struct. Mech. 2, 79–92.

[19] Szundi, I. and Stoeckenius, W. (1987) Proc. Natl. Acad. Sci. USA 84, 3681–3684.

[20] Fitter, J., Lechner, R.E., Büldt, G. and Dencher, N.A. (1996) Physica B 226, 61–65.

[21] Lechner, R.E. (1996) Neutron News 7, 9–11.

[22] Fitter, J., Lechner, R.E., Büldt, G. and Dencher, N.A. (1996) Proc. Natl. Acad. Sci. USA 93, 7600–7605.

[23] Volino, F. and Dianoux, A.J. (1980) Mol. Phys. 41, 271–279.

[24] Bee, M. (1988) Quasielastic Neutron Scattering, Adàm and Hilger, Philadelphia, PA.

[25] Varo, G. and Lanyi, J.K. (1990) Biochemistry 29, 2241–2250.

[26] König, S., Bayerl, T.M., Coddens, G., Richter, D. and Sackmann, E. (1995) Biophys. J. 68, 1871–1880.

[27] Zaccai, G. (1987) J. Mol. Biol. 194, 569–572.

[28] Papadopoulos, G., Dencher, N.A., Zaccai, G. and Büldt, G. (1990) J. Mol. Biol. 214, 15–19.

[29] Fitter, J., Lechner, R.E. and Dencher, N.A. (1997) in: Biological Macromolecular Dynamics (Cusack, S., Büttner, H., Ferrand, M., Langan, P. and Timmins, P., Eds.), pp. 123–128, Adenine Press, Schenectady, NY.

[30] Jang, D.J. and El-Sayed, M.A. (1988) Proc. Natl. Acad. Sci. USA 85, 5918–5922.

[31] Fukuda, K., Ikegami, A., Nasuda-Kouyama, A. and Kouyama, T. (1990) Biochemistry 29, 1997–2002.

[32] Varo, G. and Keszthelyi, L. (1985) Biophys. J. 47, 243–246.

[33] Le Coutre, J., Tittor, J., Oesterhelt, D. and Gerwert, K. (1995) Proc. Natl. Acad. Sci. USA 92, 4962–4966.

[34] Ganea, C., Gergely, C., Ludmann, K. and Varo, G. (1997) Biophys. J. 73, 2718–2725.

[35] Verclas, S.A.W. (1998) PhD Thesis, Universität Düsseldorf.

---

[3] Wet samples of PM films (100% r.h.) show a very similar behavior with respect to the absorption changes of the M-signal as compared to PM in solution [35].